Small sodium clusters that melt gradually: Melting mechanisms in Na_{30}

Andrés Aguado* and José M. López
Departamento de Física Teórica, Universidad de Valladolid, Valladolid 47011, Spain
(Received 5 June 2006; published 5 September 2006)

The meltinglike transition of Na_{30} is studied by orbital-free density-functional molecular dynamics simulations. The potential energy surface of Na_{30} is sampled by simulated annealing and regular quenchings performed along the dynamical trajectories. Both the ground-state structure and low-energy structural excitations are found to exhibit substantial polyicosahedral ordering. The most relevant feature of the potential energy landscape for the melting problem is the existence of many different structural isomers within an energy range of 1 meV/atom, resembling that of a glassy system (yet the structures have a high symmetry). The liquid phase is accessed gradually, with some isomerizations observed at a temperature as low as 30 K, while melting can be considered complete above approximately 200 K. The different dynamical mechanisms that allow the smooth opening of phase space available to the system as a function of temperature are identified and discussed. They can be classified in two different categories: (a) those that allow the exploration of isomers similar to the ground state, involving mainly surface isomerizations and surface melting, and leaving the structure of the cluster core unchanged; and (b) those associated with a more substantial structural change, more similar to the usual solid-solid phase transition in bulk phases; the structure of the cluster core changes only in this second type of transition. Mechanism (a) results in surface melting of the corresponding isomer upon heating; at that stage, mechanism (b) acts to transfer some excess energy from the surface to the core region, so that the surface melting is transiently avoided. Even in the fully developed liquid state, there are important differences from the bulk liquid due to the presence of the surface.

DOI: 10.1103/PhysRevB.74.115403 PACS number(s): 36.40.Ei, 36.40.Sx, 64.70.Dv, 31.15.Qg

I. INTRODUCTION

Melting is a ubiquitous phenomenon in condensed matter which, due to its cooperative nature, has no analog in microscopic systems such as diatomic molecules. It is therefore very interesting to notice that small unsupported atomic clusters, formed by only a few tens of atoms, can already show a well-defined melting transition upon heating. Understanding how cluster melting proceeds and how it is related to bulk melting is an active field of research presently. Several investigations have identified unexpected features in cluster melting. For example, Jarrold and co-workers[1] have demonstrated that small gallium and tin clusters melt at temperatures T_m higher than T_m^{bulk}, the bulk melting point. The most extensive calorimetric experiments have been performed by Haberland and co-workers, who have focused on an analysis of sodium clusters.[2–8] The most interesting observation in these studies is that the size dependence of T_m is not monotonic for Na_N clusters in the size range[3,4,6] $N \approx 50-350$ (this is not a peculiarity of sodium clusters, as it has also been observed by Breaux *et al.*[9] to happen in aluminum clusters). Combining the calorimetric determinations with a measurement of the photoelectron spectra, Haberland *et al.*[8] concluded that maxima in the latent heat q and entropy of melting Δs are correlated with *geometrical* shell closings. For smaller clusters like Na_{41}^+,[7] the experimental caloric curves do not show a well-defined melting transition but rather suggest a gradual evolution of the solid clusters toward the liquid state, spread over a very wide temperature interval. The heat capacities, determined in terms of the slope of the caloric curves, evolve continuously as a function of temperature between values typical of the solid and liquid phases, and in both low-T and high-T limits compare well with those of larger clusters showing a more abrupt melting transition. A similar conclusion has been obtained for even smaller clusters through an analysis of the temperature dependence of photoelectron spectra.[5]

Despite a number of theoretical efforts,[10–26] the intriguing melting point oscillations have not been properly interpreted by computer simulations until very recently.[27–30] By means of orbital-free molecular dynamics (OFMD) simulations, Aguado and López[27] provided a tentative explanation for the local maxima in the $T_m(N)$ curve in terms of purely geometric arguments (for some specific sizes, more compact clusters can be built, which also show an enhanced surface stability). In a separate work,[28] Aguado studied the meltinglike transition in Na_N ($N=135-147$) clusters with the OFMD method. The latent heat and entropy of melting attained a maximum at $N=147$, while T_m has a local maximum at $N=141$, both observations being in very good agreement with experiment. Noya *et al.*[29] have very recently performed a global optimization of Na clusters modeled by a parametrized potential, and found enhanced energetic stabilities for sizes which closely match the experimental latent heat maxima. The OF optimal structures[27,28] are the same as those located by Noya *et al.* for the corresponding sizes except for minor details. Finally, Chacko *et al.*[30] have simulated the melting of Na_N ($N=55,92,142$) with Kohn-Sham (KS) MD simulations and reproduced the experimental T_m values with high accuracy, although these authors ascribe more importance to electronic effects. It can therefore be concluded that most of the calorimetric results on clusters which show a well-defined melting transition are reasonably well understood now at a theoretical level. Some challenges still remain, however, such as the ground-state (GS) structure of Na_{298} which, according to the experimental photoelectron spectra,[8] is not icosahedral, or the premelting effects observed for Na_{309}.

The clusters that do not show a well-defined melting transition can be expected to fall into two different categories, on the basis of computer simulations and experimental observations. On one hand, we have so-called amorphous clusters.[19,23,25,31] As the "amorphous" attribute is presently employed in rathers loose sense when referring to clusters, it must be said that several groups consider clusters as amorphous when they show little or no discernible structural order. Aguado *et al.*[19] first proposed that a fully amorphous cluster should possess neither angular nor radial order (this last requisite being frequently overlooked as angular disorder is more easily identified by visual inspection), but obviously shows some short-range order, mostly restricted to the first coordination shell about each atom. A medium-size sodium isomer with these properties was then shown to melt gradually over a very wide temperature interval.[19] The nature of melting was seen to be essentially the analog of melting in a bulk glass. The low-temperature cluster structure is already one of the typical atomic configurations sampled in the liquid state (it can be called a "frozen liquid"). Atomic diffusion is kinetically impeded at low temperatures, and the huge number of local minima with similar amorphous features are accessed in an approximately continuous manner as the temperature is increased, because there is a correspondingly continuous distribution of free-energy barriers against diffusion. The net result is that there is not a well-defined temperature at which diffusion starts suddenly, so there is no well-defined melting point and a negligible latent heat. The nature of melting in these clusters is thus easily related to the properties of the potential energy landscape in the vicinity of the starting atomic configuration in the heating runs. Several other authors[23,25,31] have found a reduction in the latent heat as the solid and liquid structures become more similar.

Calorimetric[7] and photoelectron[5] experiments reveal that a smooth (as oppossed to abrupt) melting transition should also be expected for clusters below a small critical size, which for sodium clusters seems to be around 50 atoms (with few exceptions). It does not make much sense to define a very small cluster such as Na_{30} as amorphous, and we will see in this paper that low-energy isomers of Na_{30} have indeed a pronounced structural order. Yet the features of its potential energy landscape should be similar to those of an amorphous cluster so that the melting transition is approximately continuous. Although several computer simulations on the thermal behavior of small sodium clusters have been reported,[10–12,14,15,17,24] we believe that the dynamical mechanisms for the gradual opening of the phase space available to the cluster as a function of temperature have not been analyzed in detail yet. Some previous calculations by our own group[15] on Na_8 and Na_{20} failed to predict the correct width of the transition, as later pointed out by Vichare *et al.*[17] The main reasons for that failure are (1) the employment of a pseudopotential that did not transfer properly to cluster environments and (2) lack of ergodicity, due to computational limitations at that time. With the much more accurate energy model we have recently developed using the force-matching method[27,28] and a computationally much more efficient code, we are now in a position to simulate the melting of small clusters in a more realistic way. It is the goal of this paper to analyze in detail the melting transition in Na_{30}, providing thus not only a reproduction of the experimental trends, but also a sound explanation for them. Specifically, we will identify and classify the different dynamical mechanisms that result in the approximately continuous increase of available phase space volume with temperature. In the next section we briefly present some technical details of the method. The results are presented and discussed in Sec. III and, finally, Sec. IV summarizes our main conclusions.

II. THEORY

For a given spatial configuration of atoms, we evaluate the energy of the cluster and the force acting on each atom by employing density-functional theory (DFT) in its Hohenberg-Kohn[32] representation, where the valence electron density stands as the basic variable, thus avoiding employment of auxiliary one-particle orbitals as in its Kohn-Sham[33] representation. The details of our implementation of this so-called orbital-free DFT scheme have been described in previous work,[15,34–37] so we just present briefly the main technical issues. The electronic kinetic energy functional of the electron density is the same as in our most recent work:[27,28]

$$T_s[\rho] = T_{vW}[\rho] + T_\beta[\rho], \tag{1}$$

$$T_\beta = \frac{3}{10}\int d\vec{r}\,\rho(\vec{r})^{5/3-2\beta}\tilde{k}(\vec{r})^2, \tag{2}$$

$$\tilde{k}(\vec{r}) = (2k_f^0)^3 \int d\vec{s}\,k(\vec{s})w_\beta(2k_F^0|\vec{r}-\vec{s}|), \tag{3}$$

where $T_{vW}=\frac{1}{8}\int d\vec{r}|\nabla_\rho|^2/n$ is the von Weizsäcker functional, $k(\vec{r})=(3\pi^2)^{1/3}\rho(\vec{r})^\beta$, k_f^0 is the Fermi wave vector corresponding to a mean electron density ρ_0, $\beta=0.51$, and $w_\beta(x)$ is a weight function, determined by requiring $T_s[\rho]$ to recover the correct expression for both the uniform density and linear-response-theory limits. The mean electron density is defined as $\rho_0=V/N$, where V is the volume of a sphere of radius equal to the mean gyration radius of the cluster. The local density approximation (LDA) is used for exchange and correlation.[38,39] The ionic field acting on the electrons is represented by the local pseudopotentials of Fiolhais *et al.*[40] The parameters defining these pseudopotentials are obtained from a force-matching procedure, as explained in our recent work on Na clusters.[36] The obtained pseudopotentials are much more accurate for clusters than those originally reported by Fiolhais *et al.*,[40] which were intended to reproduce a few bulk properties under linear response theory calculations. This, together with the higher accuracy of the nonlocal kinetic energy functional as compared to semilocal approximations, has been shown to produce very accurate interatomic forces for large Na clusters.[27,28] The accuracy of our model is expected to decrease in the small size limit, however, as it can not fully reproduce electronic shell closing effects. We have checked explicitly the accuracy of our forces in simulations of Na_{30} by performing some KS calculations (see below) for configurations sampled along the MD runs. As expected, the average error increases as compared to the

large size limit, but errors in the forces remain below 10%, which is quite acceptable. While an error of this magnitude can certainly modify the predicted ground-state isomer, we will argue in the next section that this is not very relevant for the present melting study.

The cluster is placed in a unit cell of a cubic superlattice with edge 23 Å. The set of plane waves periodic in the superlattice, up to an energy cutoff of 20 Ry, is used as a basis set to expand the valence electron density. Following Car and Parrinello,[41] the coefficients of that expansion are regarded as generalized coordinates of a set of fictitious classical particles, and the corresponding Lagrange equations of motion for the electron density distribution are solved in order to determine the optimal electron density for each atomic configuration, as described in Ref. 35. Forces on atoms are then evaluated by using Hellmann-Feynman's theorem. Thus the dynamics of ions is not Car-Parrinello, but Born-Oppenheimer. The equations of motion are integrated using the Verlet algorithm,[42] with a time step of 3.5 fs. Several isokinetic MD runs were performed in order to obtain the caloric curve for each cluster. The simulated time is between 1 and 2 ns for each isokinetic run, which adds up to a total simulation time of about 45 ns, much longer than presently affordable by any other first-principles technique.

We also performed some *ab initio* KS calculations in order to check for the accuracy of the OF forces and to compare the potential energy surfaces (PESs) generated by KS and OF techniques. For these calculations, we employ the SIESTA code,[43] which is a self-consistent KS DFT method employing standard norm-conserving pseudopotentials[44] in their fully nonlocal form[45] and a flexible linear combination of atomic orbitals basis set.[46] Exchange and correlation (XC) effects are treated within the LDA, as the reference OF calculations. The basis set includes two basis functions per angular momentum channel plus one polarization orbital (DZP in the notation of Ref. 43), and the energy shift parameter[43] was kept to a value of 20 meV. The fineness of the real space grid employed to calculate Hartree and XC terms is measured by the maximum kinetic energy of the plane waves that can be represented in the grid without aliasing: a value of 40 Ry is found to give converged results. A smearing of the electron energy levels corresponding to a temperature of 100 K was applied to help convergence. All necessary convergence tests were performed.

In order to characterize the thermal properties and melting transition in Na_{30}, we have evaluated a number of different indicators, such as the caloric curve, specific heat, root-mean-square bond length fluctuation, and mean-square displacements, and studied their dependence on the kinetic cluster temperature controlled in the isokinetic ensemble. All these indicators are well known by now and have been fully described in many of our previous works.[15,34–37] To unequivocally identify the relevant dynamical processes leading to melting we have visually inspected the atom trajectories and analyzed a very powerful indicator of structural change, namely, the atomic equivalence indices[47]

$$\sigma_i(t) = \sum_j |\vec{R}_i(t) - \vec{R}_j(t)|, \tag{4}$$

where $\vec{R}_i(t)$ is the position vector of atom i at time t. In practice, we plot short-time averages of these quantities to average out the vibrational noise. These averages are taken typically over 2000 steps (that is, 7 ps). The σ_i indexes contain very detailed structural information, and are very sensitive to slight atomic rearrangements which might be overlooked in the visual inspection of MD movies and/or which do not manifest in the more global indicators mentioned above. Finally, to analyze the temperature evolution of the cluster shape, we employ the Hill-Wheeler parameters:[11] the root-mean-square radius of the cluster r, a shape deformation parameter β measuring the degree of asphericity, and another parameter γ quantifying its triaxiality. These parameters may be obtained from the three principal moments of inertia $I_1 \geqslant I_2 \geqslant I_3$, as follows:

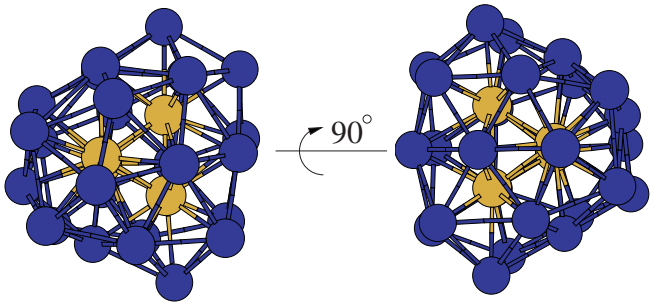

FIG. 1. (Color online) Orbital-free GS isomer of Na_{30}. Golden (light) and blue (dark) spheres differentiate atoms in core and surface regions, respectively. The four core atoms form a tetrahedron at the cluster center. Two different views, obtained by rotation of 90°, are shown to better appreciate the distorted double-icosahedron Na_{19} building blocks.

$$I_k = \frac{2}{3} r^2 \left[1 + \beta \sin\left(\gamma + \frac{(4k-3)\pi}{6} \right) \right], \tag{5}$$

$$I_1 + I_2 + I_3 = 2r^2. \tag{6}$$

$\gamma = 0$ corresponds to an axially symmetric prolate aggregate (cigarlike), while for $\gamma = \pi/3$ we have an oblate axially symmetric shape (pancake). For intermediate γ values, cluster deformation is triaxial. If $\beta = 0$, the shape is spherical and the γ parameter is meaningless. If $\gamma = \pi/3$, the maximum value of β is 0.5, corresponding to a disk of zero thickness. If $\gamma = 0$, the maximum value of β is 1, corresponding to a linear chain.

III. RESULTS

A. Structure

In order to locate the GS isomer of Na_{30}, we have performed two independent simulated annealing dynamical runs, equilibrating the cluster at a temperature of 200 K and cooling it down at a rate of 0.05 K per picosecond. In order to have a sample of relevant local minima on the PES we have additionally performed regular quenchings starting from atomic configurations sampled during the high temperature part of the simulated annealing runs. Both runs led to the same GS isomer shown in Fig. 1, and none of the quenchings was able to locate a lower-energy isomer. The

GS isomer shows a polyicosahedral packing to be energetically favored for this size. It contains four interior atoms with a slightly distorted tetrahedral structure. The rest of atoms are at the cluster surface, and are positioned in such a way that the first coordination shell of each interior atom is a slightly distorted icosahedron. Figure 1 shows that the isomer results from the combination of two 19-atom double icosahedra, rotated by approximately 90° with respect to each other.

Our finding of preferential polyicosahedral packing is in qualitative agreement with a basin hopping global optimization performed by Calvo *et al.*[48] who found evidence for this particular atomic packing employing three different energy models for Na clusters. Preference for a polyicosahedral packing has also been observed in Lennard-Jones clusters in a similar size range.[49] Nevertheless, our GS structure does not fully coincide with any of those found by Calvo *et al.* Although a direct comparison with experiment is not possible for a neutral cluster, photoabsorption experiments performed by Schmidt and Haberland[50] show that Na_{30}^{+} is triaxially deformed at a temperature of 105 K. Our GS isomer has a γ value very slightly larger than $\pi/6$ (see next section on melting), which indicates a triaxial shape with a negligibly small oblate character. Also, the photoelectron spectra of Na_N^- cluster anions measured by Kostko *et al.*[51] show the emergence of a new low-energy peak for Na_{30}^{-}, indicating an electronic shell closure for a cluster with $N_e=30$ electrons, and therefore demonstrating the breaking down of typical jellium approximations and the importance of the ionic structure at low temperatures. Although the GS structures of the neutral and cluster anion are not expected to be the same, we notice that a SIESTA local relaxation of the Na_{30} OF GS geometry shows a large gap between the highest occupied and lowest unoccupied molecular orbitals of 0.34 eV, to be compared, for example, with a gap of 0.46 eV between $N_e=8$ and 9. Our results are thus in reasonable agreement with the experimental observations around this size, and do not support the alternative structures found by Kümmel *et al.*[52] using the CAPS (cylindrically averaged pseudopotential) model, which in this size range are based on a triple icosahedron, and thus are significantly prolate deformed. At higher temperatures, where the validity of the jellium approximation is less questionable, our MD simulations (see next section) predict an increasing prolate deformation as a function of temperature. This agrees with the predictions of the jellium model for a cluster with 30 electrons.

Our melting results in the next section warn, however, against a direct comparison between the properties of the GS isomer and the results of photoabsorption or photoelectron experiments which are performed at approximately 105 K. At that temperature, we predict that several isomers and structural rearrangements will contribute to the spectra, that is, the cluster is not completely solid anymore. Moreover, our sampling of the PES reveals the existence of many structural isomers within a tiny energy range of 2 meV/atom, in line with the results found by other authors[53,54] employing more sophisticated energy models (the potential energy landscape for a Lennard-Jones cluster of this size shows also the same qualitative features[49]). We have locally optimized a group of these isomers with the SIESTA code and observed (not surprisingly) that the relative energy ordering is modified with respect to the OF calculations, but the important feature that a large number of isomers have very similar energies is maintained. The potential energy landscape is therefore found to be similar to that typical of a glassy system, a desirable property if we want to reproduce a featureless caloric curve. But the isomers found have a substantial structural order and can not be classified as amorphous. Therefore, the dynamical mechanisms leading to the gradual exploration of the PES must be different to those acting in an amorphous cluster. We will analyze those mechanisms in the next section.

An important working hypothesis in this study is that the thermal and melting properties will be most sensitive to the global feature of the potential energy landscape, namely, a large number of isomers with similar energies, rather than to the specific structure of the GS isomer. With such small energy differences, the GS structure will be nevertheless highly dependent on the energy model and/or the experimental conditions. For example, we have performed SIESTA calculations for Na_{30}^{+} and Na_{30}^{-} clusters for the same set of isomers mentioned above, and found that the energetic ordering changes as compared to the neutral clusters. Similarly, calculations performed with pseudopotentials including and neglecting nonlinear core corrections lead to different predictions. Even if the true GS isomer is ever located, it may be difficult to realize under typical experimental conditions. In summary, to fully characterize the GS structure of Na_{30} is very difficult due to the properties of its energy landscape. We can just be confident that the cluster adopts one of many polyicosahedral packings which lie very close in energy. Yet the main conclusions of this work regarding the melting transition may remain realistic because they depend on the global properties of that potential energy landscape.

B. Melting

Figure 2(a) shows the caloric curve, specific heat, rms bond length fluctuation parameter δ, and the mean-square displacements $\langle r^2(t)\rangle$ of Na_{30} as a function of increasing temperature. All indicators are suggestive of a rather gradual melting transition, although none of them provide much detailed information about the melting process. In particular, the caloric curve only shows an approximately continuous change of slope connecting the low-T and high-T heat capacity limits, in qualitative agreement with the calorimetric determinations for small sodium clusters.[7] The same is true of the fluctuations in the bond length [the small noise appreciated in the $\delta(T)$ curve gives an indication of the convergence level achieved in our MD runs]. The specific heat does show a better-defined maximum at an approximate temperature of 180 K, which correlates with a somewhat more abrupt increase in the average diffusion coefficient as obtained from the long-time slopes of the mean-square displacements. The shape of the heat capacity curve is also in agreement with those found by Lee *et al.*[24] in a similar size range, and the heat capacities in the solid and liquid regions are in quantitative agreement with experiment.[7] This supports the general validity of our OF approach, and demonstrates that the

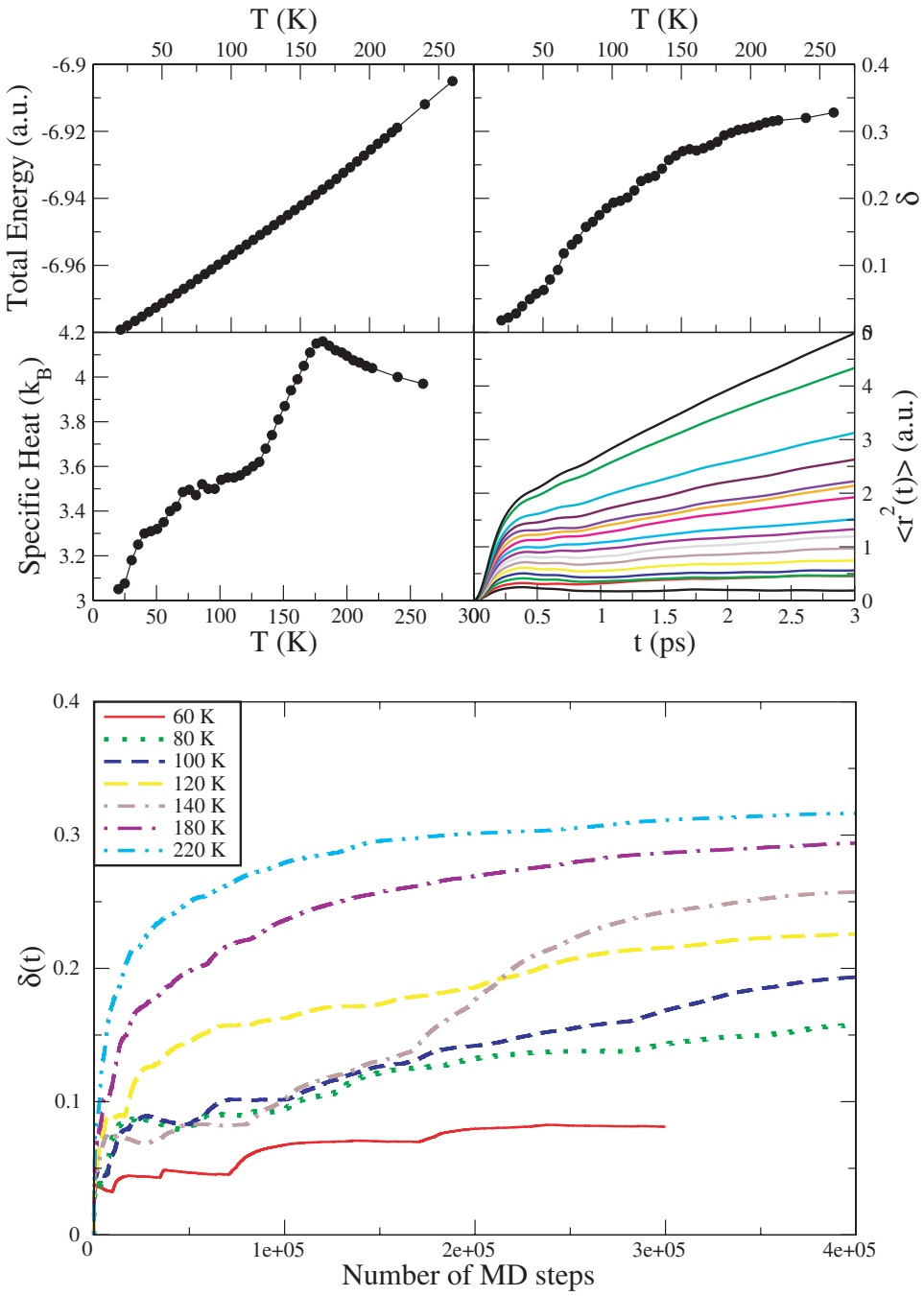

FIG. 2. (Color online) (a) Caloric curve (upper left), specific heat (lower left), rms bond-length-fluctuation parameter δ (upper right), and mean-square displacements (lower right) of Na_{30} as a function of increasing temperature. The main specific heat peak correlates with the small gap in the mean-square displacements at approximately 180 K, indicating the higher frequency of core-surface atomic rearrangements at that temperature. (b) Time evolution of the average δ parameter, with the average taken over trajectories of increasing length, for specific runs at different temperatures. This figure reveals that substantially long runs are needed to obtain reasonably converged values for δ.

failure of our initial set of simulations[15] was mostly due to the employment of a less accurate energy model (less transferable pseudopotentials and a semilocal kinetic energy functional) and to lack of ergodicity in the substantially shorter MD runs[17] performed at that time. In order to better show the improved statistical convergence, we plot in Fig. 2(b) the average values of δ parameter for several temperatures, with the averages taken over trajectory segments of increasing length. We choose δ because it is the melting indicator which converges most slowly with simulation time. It is clear from this figure that the short lengths of our previous MD runs[15] might lead to a substantial oscillatory trend in the low-temperature region of the $\delta(T)$ curve, whereas the present trajectories lead to very reasonable convergence for this melting indicator. Coupled with the much more accurate OF methodology employed here, the quality of the present results is similar to that recently found in the larger clusters.[27,28]

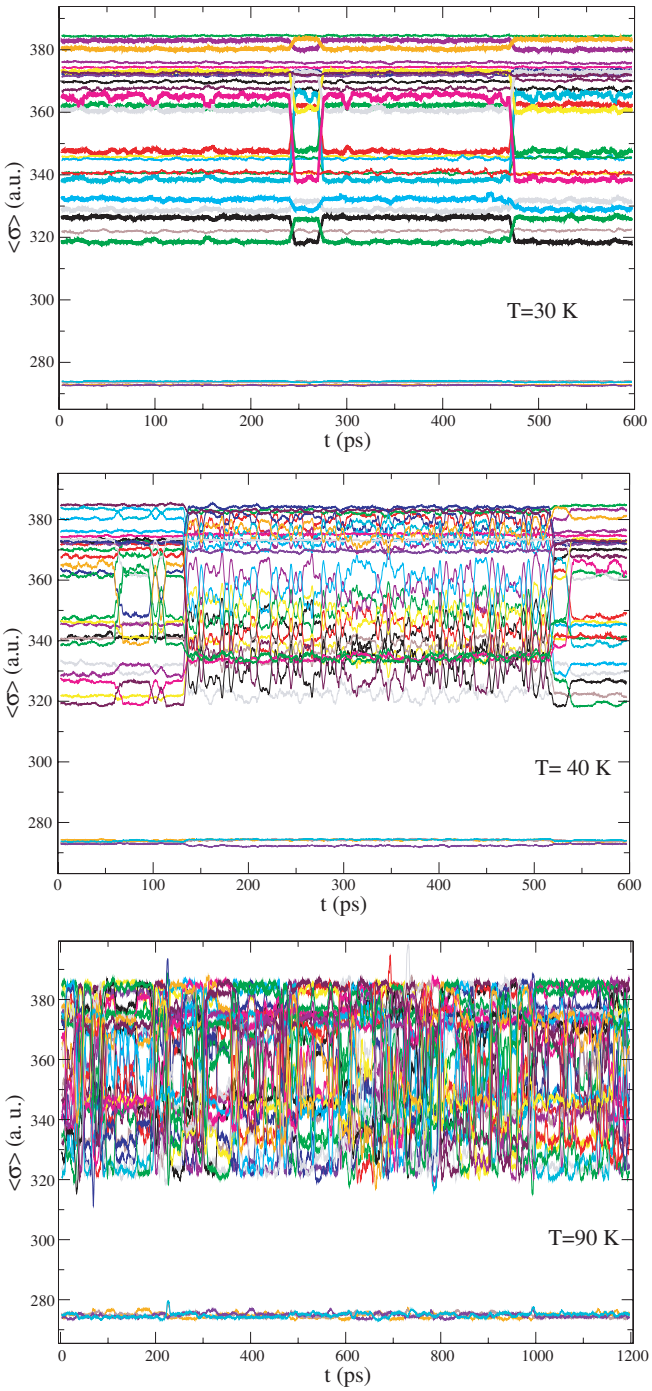

FIG. 3. (Color online) Short-time averaged atomic equivalence indices of Na_{30} in the low-temperature region: (a) 30, (b) 40, and (c) 90 K. Note that the surface shell of the GS isomer can be considered to be melted at 90 K.

Thus, even if Fig. 1 shows a well-defined structural order for Na_{30} at low temperature, the potential energy landscape shares many similarities with that of an amorphous cluster, in the sense that it can be gradually explored by the cluster as a function of increasing temperature. The rest of this section is devoted to a detailed analysis of the dynamical mechanisms by which Na_{30} explores its PES. We expect the main identified mechanisms will be qualitatively similar in most other small Na clusters.

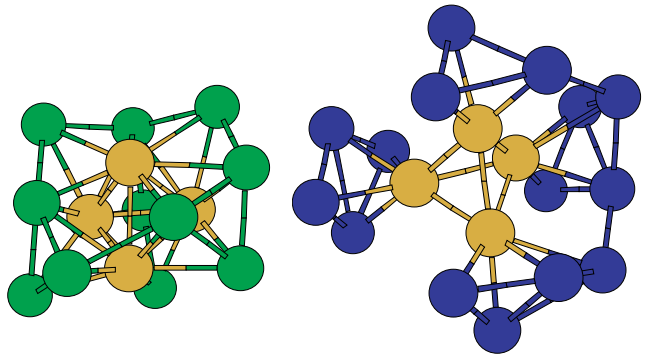

FIG. 4. (Color online) Pictorial view of the two surface atomic subshells visible in Fig. 3(a). Gold (light) spheres represent the four interior atoms adopting a tetrahedral structure. Left: atoms in the inner surface subshell are represented with green (dark) spheres. All these atoms lie on either faces or edges of the Na_4 core. Right: atoms in the outer surface subshell are represented with blue (dark) spheres. These atoms are coordinated to only one core atom each.

Figure 3 shows the atomic equivalence indices of Na_{30} for three representative runs in the low-temperature limit below 100 K. At 30 K, Fig. 3(a) shows four smaller σ values representing the tetrahedral Na_4 core identified in Fig. 1, but also shows that the surface shell can be further partiotioned into two different subshells, as characterized by the grouping of σ values. The two different surface subshells are shown in Fig. 4. The inner subshell is formed by the 11 atoms sitting on top of faces and edges of the Na_4 tetrahedron. The outer surface subshell contains 15 atoms each of them coordinated to only one atom of the Na_4 core. Thus Fig. 3(a) allows a better structural description to be performed than simple visual inspection of Fig. 1.

Figure 3(a) shows another surprising feature. At a temperature as low as 30 K, the cluster has enough energy for permutational isomerizations. By permutational we mean that the new isomer visited is topologically identical to the GS isomer, but with the identity of the atoms interchanged. The core atoms do not participate in these structural rear-

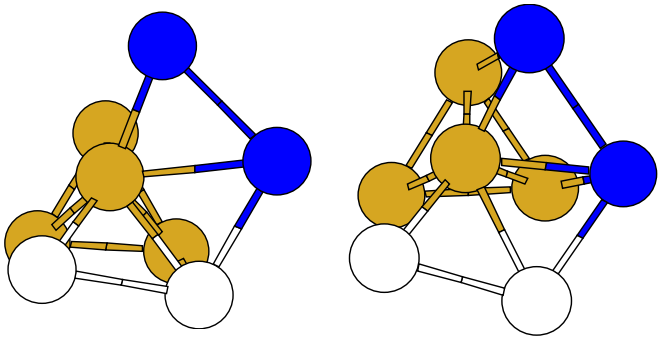

FIG. 5. (Color online) Pictorial representation of the isomerization process identified at a temperature of 30 K [see Fig. 3(a)]. Golden (light) atoms represent the inner Na_4 core. White and blue (dark) spheres represent atoms in the first and second surface subshells before the transition (left) or in the second and first surface subshells after the transition (right). Only a reduced number of atoms is shown to better visualize the nature of this transition.

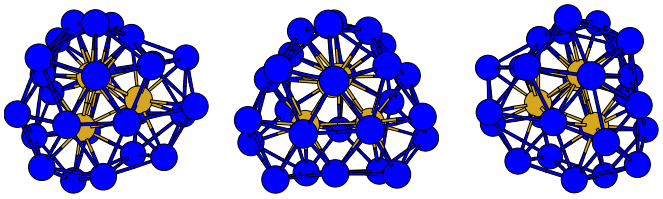

FIG. 6. (Color online) Pictorial representation of the isomerization process identified in the run at 40 K. Golden (light) and blue (dark) spheres represent core and surface atoms, respectively. The inner Na_4 tetrahedron first rotates about one edge with respect to the surface shell, which leads to a new fluctuating isomer (see text) shown in the middle part, and later on the surface rearranges (right part) to lead to an isomer equivalent to the initial one (left side).

rangements, which are further analyzed in Fig. 5. As expected, there is not enough energy available for a direct swapping of atomic positions. The mechanism for permutational isomerization is instead the concerted movement of a subset of surface atoms, which is best described as a combination of small rotation and swing movements. Through this concerted movement, surface atoms can switch between inner and outer surface subshells as a function of time, with no appreciable diffusion. These structural rearrangements have a very small associated activation barrier. Figure 5 shows only a simplified view of this process. The rest of the surface atoms also undergo small displacements that certainly contribute to the dynamical transition path. Also, we notice that we have chosen to describe this process as permutational isomerization in an operational way, although we have observed that some of these isomers are not fully equivalent to the GS. The differences are so small that even the set of σ lines is not sufficiently sensitive to them, and the energy differences obtained after local optimization are of the order of 0.03 meV/atom, so we consider all those isomers to be the same on a pragmatical basis.

At 40 K, Fig. 3(b) suggests more dramatic isomerizations are taking place. It is the first time we observe a set of apparently noisy σ lines at such a low temperature, and it took some effort for us to explain their origin. A visual representation of what is happening is offered in Fig. 6. The cage provided by the surface atoms allows for some rotational freedom of the otherwise quite rigid inner tetrahedron. This rotation is mostly performed about one of the edges of the tetrahedron, which has been chosen as perpendicular to this page in Fig. 6 to help visualization. Starting from the GS isomer (left plot), the tetrahedron rotates and adopts a new position inside the cage, with some small modifications in the surface structure (middle plot). After that, surface atoms rearrange themselves to lead again to a permutational version of the GS isomer (right plot). The new isomer shown in the middle of Fig. 6 has the strange set of σ lines shown in the middle part of Fig. 3(b). Figure 6 represents just a thermal average of the atomic positions during that part of the MD run. After analyzing more carefully the MD movies, we realized that the cluster is continuously changing between two equivalent structures where the inner tetrahedron is slightly tilted with respect to the figure shown in Fig. 6, which represents indeed a saddle point. The tilting angle can be slightly positive or negative and the middle part of Fig. 6 is

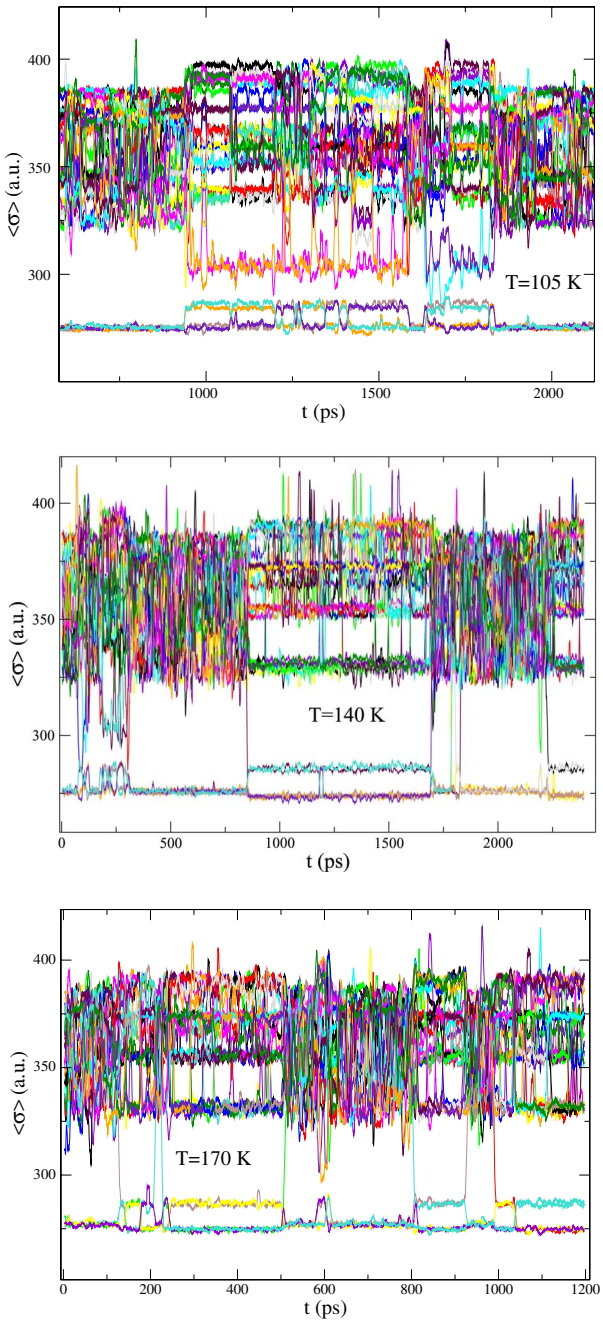

FIG. 7. (Color online) Short-time averaged atomic equivalence indices of Na_{30} in the intermediate- and high-temperature regions: (a) 105, (b) 140, and (c) 170 K. For even higher temperature, the rate of core-surface atomic rearrangements increases, but apart from that the situation is similar to that at 170 K.

the average of both structures. The new isomer is thus better described to be in a fluctuating state, similar to those observed in bulk crystalline systems such as β-quartz[55] or in high-pressure phases of BaO.[56] The two equivalent isomers can be differenciated by the identity of the σ lines, which explains the noisy pattern of Fig. 3(b). To the best of our knowledge, this is the first time a fluctuating dynamical state of this kind has been fully characterized in a small cluster.

We understand now how the floppy character of Na_{30} allows for substantial isomerization processes even at low T.

Upon increasing further the temperature up to 90 K, some new isomerization mechanisms emerge that we do not describe in detail here. The most important feature is that none of those mechanisms involve either exchange between core and surface atoms or a change of structure of the cluster core. As the isomerization rate increases with T, it finally leads to a surface-melted stage at 90 K, as shown in Fig. 3(c). Quenching runs performed at this temperature identify many different isomers, all of them based on a preferential polyicosahedral packing on top of a tetrahedral core, with energies less than 1 meV/atom above the GS. It is interesting that surface melting of this isomer at 90 K does not involve the generation of floater atoms and corresponding vacant sites at the surface, but simply proceeds from the superposition of concerted atomic rearrangements such as those discussed above.

Figure 7 shows the atomic equivalence indexes of Na_{30} in the temperature range above 100 K, for three representative runs. Just when the 90 K simulation suggested that the cluster was about to melt, a solid-solid transition is found to occur around 100 K [Fig. 7(a)]. We distinguish this transition from those observed below 100 K on the basis of the σ lines, which show that the structure of the cluster core also changes, and therefore is more similar to the solid-solid phase transformations observed in bulk phases. No core-surface atomic interchanges are nevertheless involved in this transition. The new structures stabilized at this temperature are found by quenching and shown in Figs. 8 and 9. The four inner atoms adopt now the shape of a planar rhombus (Fig. 8) or a closely related open planar structure (Fig. 9), and the surface atoms provide local icosahedral environments for those core atoms. The structure in Fig. 8 can also be visualized as a lateral coalescence of two 19-atom double icosahedra. The isomer shown in Fig. 9 can be similarly interpreted but now the main axes of the two double icosahedra are not parallel. The two structures have a sufficiently similar set of σ lines so they cannot be properly distinguished at this high temperature. An interesting feature of this transition is that it serves to transfer some energy from the surface to the core shell so that surface melting is not well developed for the new solid phase at 100 K. Surface melting is thus transiently avoided, and the new structure will have a higher thermal stability and melting point, as expected from a solid-solid transition.

In the temperature interval 100–130 K, we observe dynamical coexistence between the new isomers with the planar core and the surface-melted isomer with the tetrahedral core. The cluster fluctuates in time between these two possibilities, and spends enough time in each of them so that we could assign well-defined properties to each isomer separately. Although in a microcanonical simulation this might lead in principle to a bimodal distribution of kinetic energies and a corresponding S-shaped loop in the caloric curve, the energy difference between both isomers is so tiny (less than 1 meV/atom, and of the same order of magnitude as the energy difference between the surface melted and fully solid versions of the tetrahedral core isomer) and the melting process so gradual that the effect does not deserve further discussion in practical terms.

Starting at approximately 130 K, a new isomer with five interior atoms is accessed, as shown in Fig. 7(b). As before,

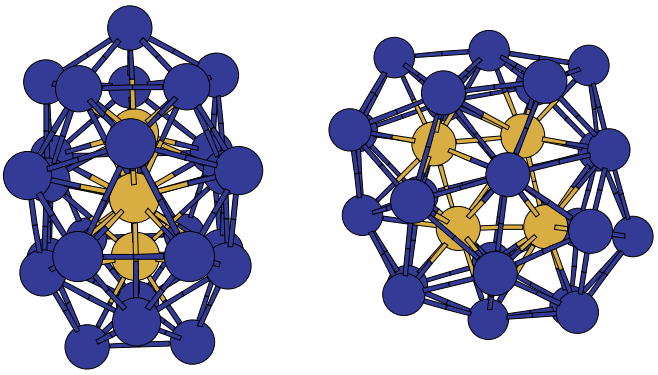

FIG. 8. (Color online) Excited-state isomer of Na_{30} visited in the temperature region about 100 K [see Fig. 7(a)]. Golden (light) and blue (dark) spheres differentiate atoms in core and surface regions, respectively. The four core atoms form a planar rhombus at the cluster center. Both front and side views are offered. The structure is again based on double-icosahedron Na_{19} building blocks, which are now "glued" laterally.

the new structure was identified by means of quenching, and is shown in Fig. 10 from several perspectives. The five core atoms adopt the structure of a trigonal bipyramid, and the local coordination shell about these five atoms continues to be a distorted icosahedron. There appears again a dynamic coexistence regime between isomers with five and four interior atoms, through which interchange of atoms between core and surface shells can occur for the first time in the heating process. The new isomer is also seen to have a thermally more stable surface shell, and during the time intervals spent in its catchment basin, surface melting is not so clearly established as for the isomers with a four-atom core. In this range of temperatures, generation of floater atoms is also possible, although they exist just for a very short time and cannot diffuse very far from the place where they were created. This can be seen in the σ lines which temporarily adopt abnormally high values in Fig. 7(b).

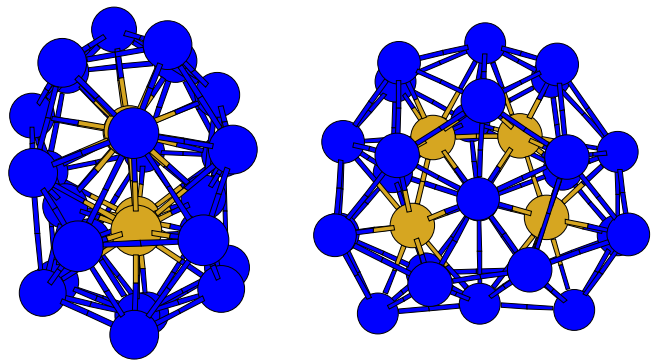

FIG. 9. (Color online) Excited-state isomer of Na_{30} visited in the temperature region about 120 K (it has a similar set of σ lines as that shown in the previous figure). Golden (light) and blue (dark) spheres differentiate atoms in core and surface regions, respectively. The four core atoms adopt an open planar structure at the cluster center. The structure can also be seen as a decorated pentagonal bipyramid Na_7 (right part). The local environment of each inner atom is again icosahedral.

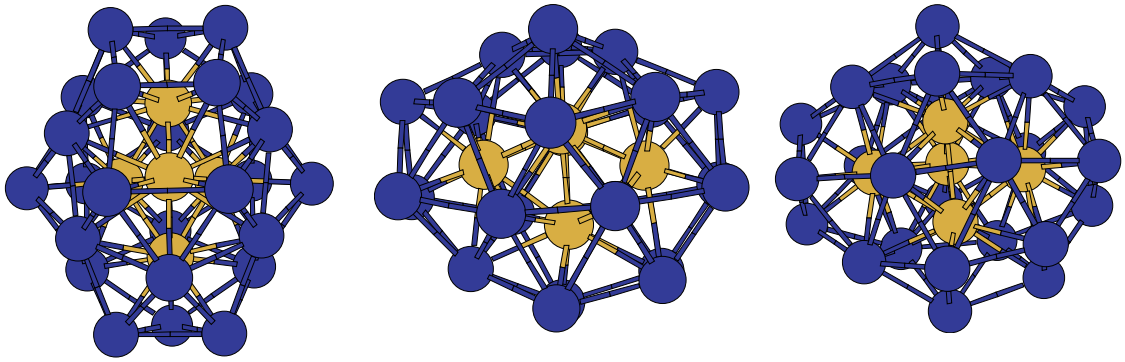

FIG. 10. (Color online) Three different views of the excited-state isomer of Na_{30} visited in the temperature region starting at about 130 K. Golden (light) and blue (dark) spheres differentiate atoms in core and surface regions, respectively. There are five core atoms which adopt a trigonal bipyramidal structure. The local environment of each inner atom is again icosahedral.

Upon further temperature increase, nothing really new happens, but the rate at which the several rearrangement processes discussed so far occur steadily increases [Fig. 7(c)]. At approximately 180 K, the rate of core-surface intershell diffusion increases in a more marked way (Fig. 2) and the surface melting is complete irrespective of the number of core atoms, which explains the main peak in the heat capacity. But even at a temperature of 250 K (not explicitly shown), the usual picture of a bulk liquid can not be fully recovered, simply because a bulk liquid is a homogeneous system and a cluster is not. The rate of core-surface diffusion remains substantially lower than that of surface diffusion.

Finally, we show in Fig. 11 the temperature evolution of the Hill-Wheeler shape parameters. The cluster radius r is seen to increase substantially at the first solid-solid transformation, as well as the asphericity parameter β, but the triaxiality of the cluster is maintained. The isomers shown in Figs. 8 and 9 are therefore significantly less compact and less spherical than the GS isomer. The isomer shown in Fig. 10 is, however, relatively more compact and shows a prolate deformation, which explains the abrupt decrease in γ at about 130 K. Our high-T OF results are thus in agreement with the jellium model which predicts a prolate deformation for a cluster with 30 electrons. The cluster shape remains nevertheless substantially triaxial in character, as γ values are always close to $\pi/6$.

IV. CONCLUSIONS

In this work, we have reported first-principles MD simulations of the melting process in a small Na_{30} cluster. A preliminary exploration of the potential energy surface shows the presence of many structural isomers within an energy range of the order of 1 meV/atom, all of them based on preferential polyicosahedral packing, thus resembling a potential energy landscape typical of glassy systems. Nevertheless, these structures cannot be classified as amorphous, as we have shown them to possess both a high symmetry and radial order. Our simulations reproduce the experimental observation[7] that small sodium clusters melt gradually over a very wide temperature interval, with no abrupt features appreciable in the caloric curve and thus with a negligibly small latent heat. The main goal of this study has been to identify and classify the dynamical mechanisms which allow the smooth opening of phase space available to the system as its temperature is increased. After analyzing all those mechanisms, we have essentially classified them in two different categories. (a) On one hand are all those that allow the exploration of isomers similar to the ground state. These mechanisms operate at low temperatures, and are already active at 30 K. They mainly involve concerted surface rearrangements, changes in the relative orientation of core and surface shells, and also surface melting, when they happen at a sufficiently high rate. (b) On the other hand, those mechanisms associated with a more substantial structural change begin to be important at approximately 100 K. They are the analog of the solid-solid phase transformations found in many bulk crystals, and involve the concerted rearrangement of all atoms, including those forming the inner core shell. Mechanism (a) can only lead to surface melting of the corresponding isomer. We have made the interesting observation that mechanism (b) is more likely to act once the cluster has attained a surface melting stage. At that point, a solid-solid

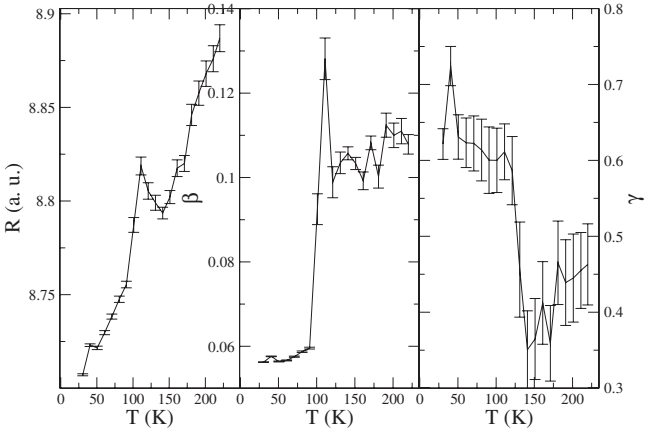

FIG. 11. Temperature evolution of the mean square radius r (left), asphericity parameter β (middle), and triaxiality parameter γ (right) of Na_{30}. Error bars are covariances of cluster shape parameters.

transition is able to efficiently transfer energy from the surface to the core region so that the surface melting stage is transiently avoided. Some of these solid-solid transformations can also induce the exchange of atoms between surface and core radial shells. The rate of core-surface atom exchange steadily increases with temperature leading to complete melting, but it always remains lower than the surface diffusion rate. This is in contrast with a homogeneous bulk liquid but in line with the behavior observed in heterogeneous liquid-vapor bulk interfaces.[57]

ACKNOWLEDGMENTS

This work was supported by the EU-FEDER Program, the Ministerio de Educación y Ciencia (Grant No. MAT2005-03415), and the "Ramón y Cajal" program.

*E-mail address: aguado@metodos.fam.cie.uva.es

[1] A. A. Shvartsburg and M. F. Jarrold, Phys. Rev. Lett. **85**, 2530 (2000); G. A. Breaux, R. C. Benirschke, T. Sugai, B. S. Kinnear, and M. F. Jarrold, *ibid.* **91**, 215508 (2003).
[2] M. Schmidt, R. Kusche, W. Kronmüller, B. von Issendorff, and H. Haberland, Phys. Rev. Lett. **79**, 99 (1997).
[3] M. Schmidt, R. Kusche, B. von Issendorff, and H. Haberland, Nature (London) **393**, 238 (1998).
[4] R. Kusche, Th. Hippler, M. Schmidt, B. von Issendorff, and H. Haberland, Eur. Phys. J. D **9**, 1 (1999).
[5] M. Schmidt, C. Ellert, W. Kronmüller, and H. Haberland, Phys. Rev. B **59**, 10970 (1999).
[6] M. Schmidt and H. Haberland, C. R. Phys. **3**, 327 (2002).
[7] M. Schmidt, J. Donges, Th. Hippler, and H. Haberland, Phys. Rev. Lett. **90**, 103401 (2003).
[8] H. Haberland, Th. Hippler, J. Donges, O. Kostko, M. Schmidt, and B. von Issendorff, Phys. Rev. Lett. **94**, 035701 (2005).
[9] G. A. Breaux, C. M. Neal, B. Cao, and M. F. Jarrold, Phys. Rev. Lett. **94**, 173401 (2005).
[10] U. Röthlisberger and W. Andreoni, J. Chem. Phys. **94**, 8129 (1991).
[11] A. Bulgac and D. Kusnezov, Phys. Rev. Lett. **68**, 1335 (1992); Phys. Rev. B **45**, 1988 (1992).
[12] N. Ju and A. Bulgac, Phys. Rev. B **48**, 2721 (1993).
[13] P. Blaise, S. A. Blundell, and C. Guet, Phys. Rev. B **55**, 15856 (1997).
[14] A. Rytkönen, H. Häkkinen, and M. Manninen, Phys. Rev. Lett. **80**, 3940 (1998); Eur. Phys. J. D **9**, 451 (1999).
[15] A. Aguado, J. M. López, J. A. Alonso, and M. J. Stott, J. Chem. Phys. **111**, 6026 (1999).
[16] F. Calvo and F. Spiegelmann, Phys. Rev. Lett. **82**, 2270 (1999); J. Chem. Phys. **112**, 2888 (2000).
[17] A. Vichare, D. G. Kanhere, and S. A. Blundell, Phys. Rev. B **64**, 045408 (2001).
[18] A. Aguado, J. M. López, J. A. Alonso, and M. J. Stott, J. Phys. Chem. B **105**, 2386 (2001).
[19] A. Aguado, L. M. Molina, J. M. López, and J. A. Alonso, Eur. Phys. J. D **15**, 221 (2001).
[20] J. A. Reyes-Nava, I. L. Garzón, and K. Michaelian, Phys. Rev. B **67**, 165401 (2003).
[21] F. Calvo and F. Spiegelmann, J. Chem. Phys. **120**, 9684 (2004).
[22] K. Manninen, A. Rytkönen, and M. Manninen, Eur. Phys. J. D **29**, 39 (2004).
[23] K. Manninen, H. Häkkinen, and M. Manninen, Phys. Rev. A **70**, 023203 (2004).
[24] M. Lee, S. Chacko, and D. G. Kanhere, J. Chem. Phys. **123**, 164310 (2005).
[25] K. Manninen, A. Rytkönen, and M. Manninen, Comput. Mater. Sci. **35**, 158 (2006).
[26] M. Itoh, V. Kumar, and Y. Kawazoe, Phys. Rev. B **73**, 035425 (2006).
[27] A. Aguado and J. M. López, Phys. Rev. Lett. **94**, 233401 (2005).
[28] A. Aguado, J. Phys. Chem. B **109**, 13043 (2005).
[29] E. G. Noya, J. P. K. Doye, D. J. Wales, and A. Aguado, cond-mat/0506329 (unpublished).
[30] S. Chacko, D. G. Kanhere, and S. A. Blundell, Phys. Rev. B **71**, 155407 (2005).
[31] E. G. Noya, J. P. K. Doye, and F. Calvo, Phys. Rev. B **73**, 125407 (2006).
[32] P. Hohenberg and W. Kohn, Phys. Rev. **136**, 864B (1964).
[33] W. Kohn and L. J. Sham, Phys. Rev. **140**, 1133A (1965).
[34] A. Aguado, L. E. González, and J. M. López, J. Phys. Chem. B **108**, 11722 (2004).
[35] A. Aguado, D. J. González, L. E. González, and J. M. López, *Progress in Chemical Physics Research* (Nova Science Publishers, New York, in press).
[36] A. Aguado and J. M. López, Phys. Rev. B **71**, 075415 (2005).
[37] A. Aguado and J. M. López, J. Chem. Theory Comput. **1**, 299 (2005).
[38] J. P. Perdew and A. Zunger, Phys. Rev. B **23**, 5048 (1981).
[39] D. M. Ceperley and B. J. Alder, Phys. Rev. Lett. **45**, 566 (1980).
[40] C. Fiolhais, J. P. Perdew, S. Q. Armster, J. M. MacLaren, and M. Brajczewska, Phys. Rev. B **51**, 14001 (1995); **53**, 13193 (1996).
[41] R. Car and M. Parrinello, Phys. Rev. Lett. **55**, 2471 (1985); M. C. Payne, M. P. Teter, D. C. Allan, T. A. Arias, and J. D. Joannopoulos, Rev. Mod. Phys. **64**, 1045 (1992).
[42] L. Verlet, Phys. Rev. **159**, 98 (1967); W. C. Swope and H. C. Andersen, J. Chem. Phys. **76**, 637 (1982).
[43] J. M. Soler, E. Artacho, J. D. Gale, A. García, J. Junquera, P. Ordejón, and D. Sánchez-Portal, J. Phys.: Condens. Matter **14**, 2745 (2002).
[44] D. R. Hamann, M. Schlüter, and C. Chiang, Phys. Rev. Lett. **43**, 1494 (1979).
[45] L. Kleinman and D. M. Bylander, Phys. Rev. Lett. **48**, 1425 (1982).
[46] E. Anglada, J. M. Soler, J. Junquera, and E. Artacho, Phys. Rev. B **66**, 205101 (2002).
[47] V. Bonacić-Koutecký, J. Jellinek, M. Wiechert, and P. Fantucci, J. Chem. Phys. **107**, 6321 (1997); D. Reichart, V. Bonacić-Koutecký, P. Fantucci, and J. Jellinek, Chem. Phys. Lett. **279**, 129 (1997).
[48] F. Calvo, S. Tran, S. A. Blundell, C. Guet, and F. Spiegelmann, Phys. Rev. B **62**, 10394 (2000).
[49] D. D. Frantz, J. Chem. Phys. **115**, 6136 (2001).

[50] M. Schmidt and H. Haberland, Eur. Phys. J. D **6**, 109 (1999).
[51] O. Kostko, N. Morgner, M. Astruc Hoffmann, and B. von Issendorff, Eur. Phys. J. D **34**, 133 (2005).
[52] S. Kümmel, M. Brack, and P. G. Reinhard, Phys. Rev. B **58**, R1774 (1998); **62**, 7602 (2000).
[53] L. Kronik, I. Vasiliev, and J. R. Chelikowsky, Phys. Rev. B **62**, 9992 (2000); L. Kronic, I. Vasiliev, M. Jain, and J. R. Chelikowsky, J. Chem. Phys. **115**, 4322 (2001).
[54] I. A. Solov'yov, A. V. Solov'yov, and W. Greiner, Phys. Rev. A **65**, 053203 (2002).
[55] Y. Ma and S. H. Garofalini, Phys. Rev. B **73**, 174109 (2006).
[56] A. Aguado, L. Bernasconi, and P. A. Madden, J. Chem. Phys. **118**, 5704 (2003).
[57] A. Aguado, M. Wilson, and P. A. Madden, J. Chem. Phys. **115**, 8603 (2001).